FORMATION AND MORPHOLOGICAL CHANGES OF STRESS ACTIN FILAMENTS IN ADIPOSE-DERIVED STEM CELLS

By

Adam Jordan Priester

Presented to the Faculty of the Graduate School of

The University of Texas at Arlington

Submitted in Partial Fulfillment of the Requirements for the Degree of

Master of Science in Biomedical Engineering

Supervising Professor:

Michael Cho, Ph.D.

THE UNIVERSITY OF TEXAS AT ARLINGTON

December 2023

ABSTRACT

Formation and Morphological Changes of Stress Actin Fibers in Adipose-Derived Stem Cells

Adam Jordan Priester

The University of Texas at Arlington

Supervising Professor: Michael Cho

Adipose-Derived Stem Cells (ADSCs) are a sub-type of stem cell that can be collected and isolated from the adipose tissue. Adipogenesis describes the commitment and differentiation of stem cells, including ADSCs, toward the adipocyte lineage. While much research has been completed on this process in the long term (>2 weeks), morphological changes of adipogenesis during the early phase (<24 hours) are lacking in the literature and remain to be elucidated. The current study focuses on these changes in the early and later stages of adipogenesis using adipogenic differentiation factors and fluorescent imaging analyses. Quantifiable data on morphological changes during both phases can provide insight into how these changes affect later differentiation and lay the groundwork for additional research in this area.

Using fluorescent image analysis, it was shown that the eccentricity of ADSCs, a measure of cellular circularity, decreases exponentially in the early phase of adipogenesis. The cellular area appears to increase exponentially during the same early period. During the later stages of differentiation, it was shown that actin filament length decreases exponentially and the ratio of lipid to actin length increases exponentially, demonstrating that lipid accumulation outpaces actin filament shortening and increasing circularity during the later stages. These findings may be used in future studies to further define the role of actin filament-mediated morphological changes and mechanobiology during adipogenesis.

COPYRIGHT

ACKNOWLEDGEMENTS

I would like to express my gratitude to the following people:

My supervising professor and committee member, Dr. Michael Cho for his guidance, advice, knowledge, and overall mentorship through the completion of my work.

My lab members, Dr. Nagham Alatrash, Dr. Rafiul Shihab, Ms. Anne Alsup, Mr. Zachary Armstrong, Mrs. Kelli Fowlds, and Ms. Mia Grubbs for their generous help and support in the completion of my work.

To Drs. Alan Bowling and Hyejin Moon and the National Institutes of Health, for financial support which made this research possible.

DEDICATION

I would like to dedicate this work to my immediate family and close friends. Their support and understanding have encouraged me to continue and complete this work. They have been a great support system and I could not have done it without them, so for that, I am thankful to each one of them.

TABLE OF CONTENTS

TABLE OF FIGURES

Figure 4-1: Single ADSC viewed at 60x magnification at various times post-seeding. All images were produced at 60x magnification. Nascent actin filaments are show in red via phalloidin x Texas Red stain. a) 2 hours: Cells have recently attached and are round in shape (eccentricity ~1) under microscope. b) 4 hours: Cells are still generally round but begin to increase in area. c) 12 hours: From hour 4 to hour 12, cellular area nearly triples, and eccentricity decreases. d) 24 hours: Increase of cellular area effectively stops, and eccentricity is approximately half that of hour 12. At the higher timepoints, each cell has dozens of processes extending from the main cell body, causing a large variation in both eccentricity and area.

Figure 4-2: Calculated eccentricity of ADSCs (+/- S.D.) within 24 hours post-seeding according to Equation 1. Eccentricity greatly decreases from hour 2 to hour 4, with the decrease continuing at a slower rate in the following timepoints. *$p < 0.05$ compared to hour 2.

Figure 4-3: Measured area of ADSCs (+/- S.D.) within 24 hours post-seeding. There is a marked increase between one timepoint and the subsequent timepoint up to hour 12. Between hours 12 and 24, the increase plateaus. *$p < 0.05$ compared to hour 2.

Figure 4-4: Normalized measured eccentricity and area of ADSCs (+/- S.D.) within 24 hours post seeding. Normalization is necessary due to the high variability in cell size and eccentricity making comparison to hour 2 difficult. The best fit curve for area data is linear, and the best fit for eccentricity data is exponential. The two curves intersect at approximately day 14. *$p < 0.05$ compared to hour 2.

Figure 4-5: ADSCs at 60x magnification 5 days after seeding. No data was collected between hour 24 and day 5 due to experimental limitations. Nuclei are stained blue, actin filaments are stained red, and lipids are stained green. The white bar is parallel to and just below a single actin

filament used for calculations. After 5 days, actively differentiating cells begin to lose the linear shape seen after 24 hours and can be seen to begin rounding.

Figure 4-6: ADSCs at 60x magnification 10 days after seeding. Nuclei are stained blue, actin filaments are stained red, and lipids are stained green.

Figure 4-7: Actin filament length across 12 days of differentiation measured using NIS-Elements software. An exponential curve was fitted to this data. The length begins at day 5 around 30 μm^2 and decreases approximately according to the curve until day 12. Actin length decreases over this period because ADSCs are becoming rounder.

Figure 4-8: Experimental lipid accumulation divided by actin filament length, normalized by cell count across 12 days of differentiation. Lipid accumulation was found using LipidTox™. Normalization was needed as eccentricity could not be found due to high cell density.

CHAPTER 1:

Introduction

1.1 Adipose-Derived Stem Cells

Adipose derived stem cells (ADSCs) are a sub-type of stem cell that is collected from adult adipose tissue.[1] Specifically, these cells are collected from normal (non-diabetic) human subjects during elective liposuction surgery.[2] ADSCs can be induced to differentiate into several distinct phenotypes, dependent on multiple factors such as biological factors supplied to the cells or external forces (mechanical flow, etc.) placed on them.[3,4] In both regenerative medicine and tissue engineering, ADSCs are a valuable cell source because of the large quantity of adipose tissue in adult patients compared to cord blood or bone marrow.

Adipogenesis is the commitment and differentiation of stem cells toward the adipocyte lineage.[5,6] During this process, individual stem cells decrease in overall cell volume and become more rounded in shape.[7] Interestingly, contact with the appropriate biological factors does not guarantee differentiation of all stem cells into adipocytes. Multiple factors including substrate stiffness, cellular morphology, and cell density have been shown to affect the process.[8] In past studies, successful adipogenesis was indicated by accumulation of lipids within the cell.[9,10]

1.2 G-actin and F-actin Structure/Assembly

Actin filaments (also referred to as microfilaments) comprise the majority of a cell's cytoskeleton, constituting about 20% of the total cellular protein content.[11] In their polymeric form, they are thin, flexible rods that are able to form complex networks.[12,13] Cortical actin comprises a thin network just inside the cell membrane.[14] Stress actin forms contractile networks that are more involved in cellular motility and adhesion.[15,]

The actin monomer (G-actin) is comprised of a 375 amino acid polypeptide chain folded into two α/β domains. As shown in Figure 1-1, these monomers bind to the fast-growing barbed (or +) end of the polymeric actin filaments (F-actin) after formation of dimers/trimers following activation by ATP binding. F-actin forms a right-handed, two-chained helix, with approximately 13 molecules repeating every six turns. At the pointed (or -) end of an F-actin polymer, hydrolysis of ATP to ADP takes place due to the ATPase activity of the filament.[17,18] Due to the low stability of ADP F-actin, the monomers at this end of the filament dissociate, and free G-actin is made available to recycle into new filaments.

1.3 Actin Function

The "treadmilling" of actin filaments is the basis for which cells are able to perform several vital functions such as migration of the cell as a whole, movement of intracellular components, and division.[19] One function of particular interest of treadmilling is adhesion of cells to a substrate, as cells search for a configuration that is optimal for their viability. When cells are introduced into a new environment (e.g., seeding onto glass or a polymer), actin filaments within the cell form extensions at the boundary to prod the surface. Once one of these extensions reaches a suitable length and position, polymerization of the filament is stopped by an actin-capping protein (Figure 1-2).[20,21] This cessation of growth of actin filaments is tantamount to all of the previously mentioned cellular functions, including cellular adhesion.

Investigation into actin filament growth during the initial adhesion period could provide insight into cells' ability to differentiate in later stages. For instance, in the later window, the length of the filaments relates to cells' progression in the adipocyte lineage. This is valuable

information as premature removal of the cells from growth media would cut short many of the cells' differentiation, hindering their use in the fields of tissue engineering and regenerative medicine.[22] Furthermore, a better understanding of morphological changes in stem cells either in the early or later stages of adipogenesis could lead to the development of differentiation protocols that can maximize the yield of stem cell differentiation and therefore increase the stem cell therapeutic potency.

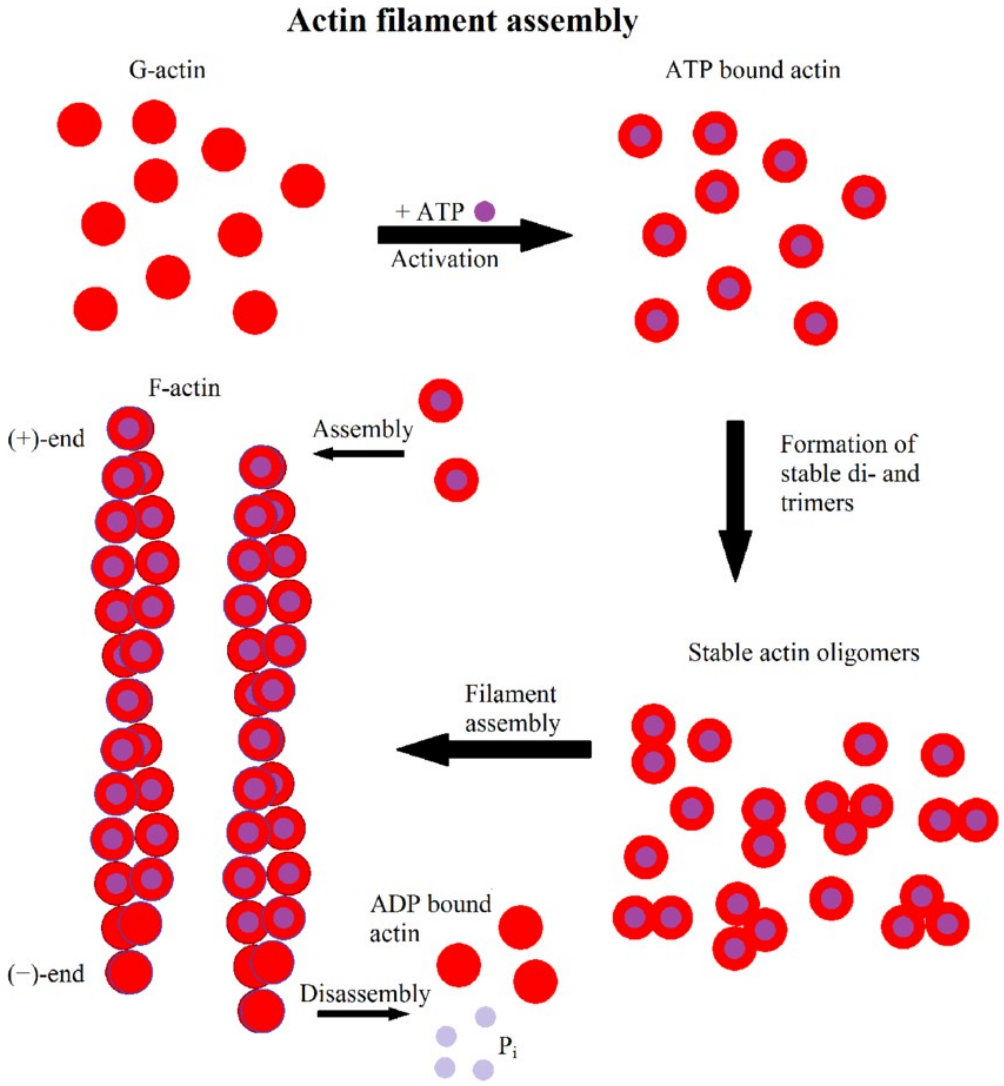

Figure 1-1: Scheme of F-actin formation. Monomers of ATP-bound G-actin are added to di- and trimers of G-actin to form F-actin filaments. The (+)-end of the filament is the end to which new oligomers are added, and the (-)-end is either stable or disassembled. The now ADP-bound actin monomers are free for activation and addition to new filaments.

[Reference: https://www.researchgate.net/publication/332515317_The_Cytoskeleton-A_Complex_Interacting_Meshwork]

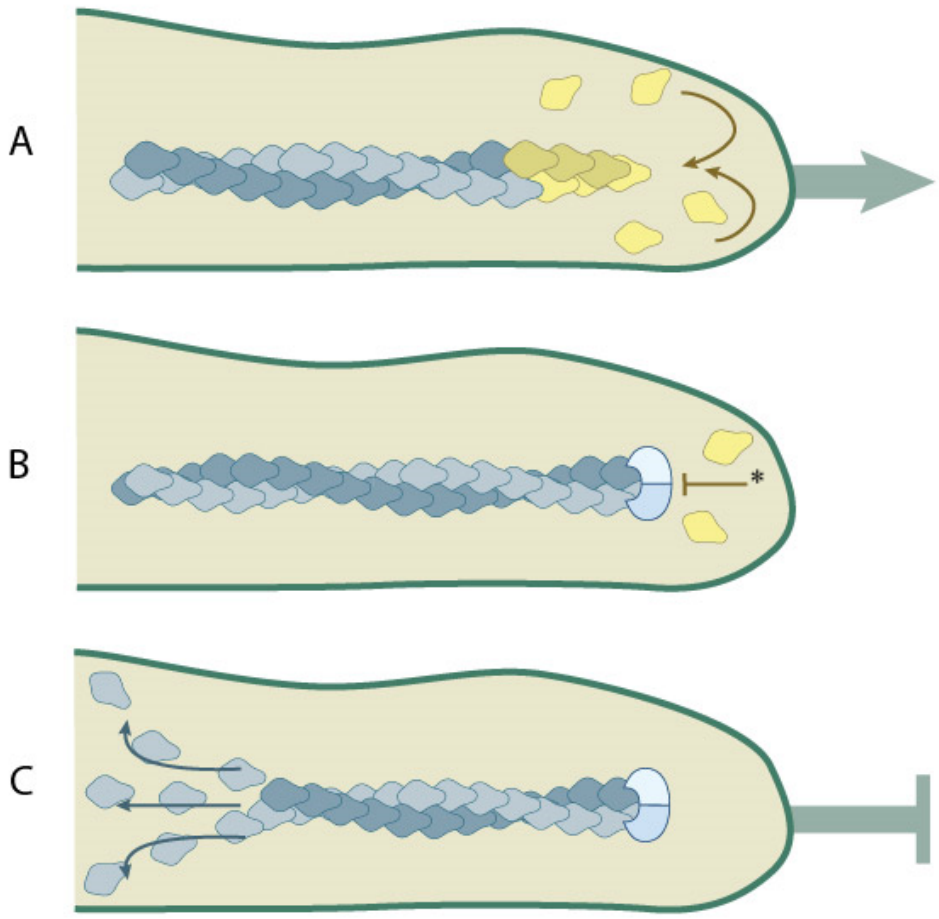

Figure 1-2: Actin capping protein mechanism. Cells use F-actin filaments to extend processes, portions of the cell membrane that jut from the main cell body, as a means of migration. Actin capping proteins are used to stop the growth of these processes once they reach the desired length. (A) Free G-actin monomers (yellow) bind to the (+) end of a growing actin filament (blue) within a cellular process. (B) Intracellular signals initiate the binding of a capping protein (*) to the (+) end of the filament which prevents new monomers from binding. (C) The capping protein stops the process from growing further. The (-) end of the filament disassembles, producing free G-actin monomers.

[Reference: https://www.mechanobio.info/cytoskeleton-dynamics]

CHAPTER 2:

Rationale/Overall Hypothesis

The first specific aim of this work is to elucidate the changes of ADSC morphology within the first 24-hour period of adipogenesis. Extensive work has been done in the literature with respect to stem cell differentiation. Recent biotechnical advances have made this differentiation both regulatable and reproducible in the lab. Much of this work focuses on F-actin structures within the cell. Despite the abundance of data available, past experiments have focused on the longer-term (days to weeks) window and an insufficient amount of data has been reported in the literature during the initial seeding period. More investigation into the dynamics of F-actin structures in this period is valuable, as the early arrangement of these fibers serves as a basis for later, more complex arrangements. Past work has been done to model the forces exerted on actin structures within the cells as they differentiate along various lineage pathways, but again has primarily focused on time periods greater than 24 hours. The focus of this study is to visualize and quantify the arrangements of F-actin fibers in the early stage.

The second specific aim of this study is to relate the changes of F-actin within ADSCs to the progress of adipogenic differentiation in a longer, 12-day period after seeding. It is interesting to note that stem cells become round adipocytes at the later stages of adipogenesis, suggesting there is correlation between the cell morphology and the extent of adipogenesis at different times. This aim is completed by estimating the cell morphology by the length of stress microfilaments and correlating it with the accumulation of lipids in the cells. Differentiation of multiple stem cell types, including ADSCs have been extensively studied since the 1970s.[23]

However, the majority of this work has been focused on bone marrow-derived mesenchymal stem cells. As ADSCs originate from white adipose tissue, they are strong candidates for regeneration of soft tissue, as previous studies have shown that they exhibit low immunogenicity after differentiation.[24,25] New insight into the morphological changes of ADSC actin filaments during differentiation may prove useful in clinical roles.

CHAPTER 3:

Materials and Methods

3.1 Growth and Differentiation of Adipose-Derived Stem Cells

Human adipose-derived stem cells (Lonza) were used for this study at passages 5-11. A culture medium (Lonza) consisting of ADSC Basal Media and ADSC-GM Singlequots™ Supplement Kit containing 10% Fetal Bovine Serum, 2% L-glutamine, and 0.02% gentamycin were used to culture cells. Cells were seeded at 1 x 10^6 cells in a 25 cm^2 flask and allowed to reach confluence. Cells were dissociated using 0.25% EDTA-1mM Trypsin (Lonza) and seeded at ~250 cells/cm^2 on 15 mm glass bottom culture dishes and incubated at 37 °C for 2, 4, 6, 12, and 24 hours for short-window adhesion analysis.

For longer-window adhesion analysis, cells were seeded using the same method at a density of 2.5 x 10^4 cells/cm^2 and incubated under the same conditions as the short-window cells for 5, 7, 9, and 12 days. Approximately 24 hours after seeding, normal media was aspirated and replaced with 200 µL adipogenic induction media to induce differentiation. This induction media contains 1 mM dexamethasone, 10 mg/ml insulin, 200 mM indomethacin and 0.5 mM isobutylmethylxanthine. Adipogenic induction media was replaced every 2 days.

3.2 Fluorescence Microscopy

For the short-window samples, the media was removed after each incubation period, and cells were stained with 6 µM Texas Red™ x Phalloidin solution (Lonza) to visualize F-actin and incubated at 37 °C for 10 minutes. After incubation, the cells were washed three times using PBS

with Mg^{2+}/Ca^{2+}. Cells were imaged using a Nikon**:** Ti Series inverted microscope and its associated NIS-Elements software at 60x magnification.

For the longer-window samples, media was removed from the dishes on each specified day and cells were stained with NucBlue™ Live ReadyProbes™ Reagent (ThermoFisher) and incubated at 37 °C for 10 minutes. After washing, the cells were stained with 1x Texas Red™ x Phalloidin solution (Lonza) and incubated at 37 °C for 10 minutes. Finally, after another round of washing, cells were stained with 1x LipidTox™ Neutral Cell Lipid Stain (ThermoFisher) and incubated at room temperature for 30 minutes. After this final incubation, cells were immediately imaged using the Nikon: Ti Series microscope at 60x magnification.

3.3 Cell Area, Eccentricity, and Fluorescence Analysis

To interpret experimental results, several image processing applications were used. To determine cell area, length, and F-actin fluorescence, software associated with the Nikon microscope was used (NIS-Elements). For the short-window samples, a total of 10 images were taken from each sample, for a total of 60 images. An individual cell from each image was analyzed, with the background removed. To visualize overall F-actin fluorescence, cells were observed using the Texas Red Channel of the application. Cells were selected using the application's region of interest (ROI) function, which computed the selection's area in μm^2. To find cellular eccentricity, the major and minor axes of the cells were measured using the Measurement function. As defined in Equation 3-1, cellular eccentricity is equal to the length of the minor axis (m_l) divided by the length of the major axis (M_l). These data were imported to Microsoft Excel for further analysis. An individual cell from each image was analyzed, with contrast increased and the background removed.

$$E = \frac{m_l}{M_l}$$

Equation 3-1: Cellular eccentricity calculation. E = eccentricity, m_l = minor axis length, M_l = major axis length.

For the longer time window samples, the NIS-Elements software was again used to determine the fluorescence of lipids (green) and fluorescence of actin (red). The software also provided fluorescence data of nuclei (blue), so that the cells could be easily identified. The Measurement function was used to manually find the length of individual F-actin filaments in representative cells. The green and red intensities for at least 8 sample cells for each day were collected, with two trials being run. Fluorescence intensity and actin filament length data was then exported to Excel for further analysis (Figure 3-1).

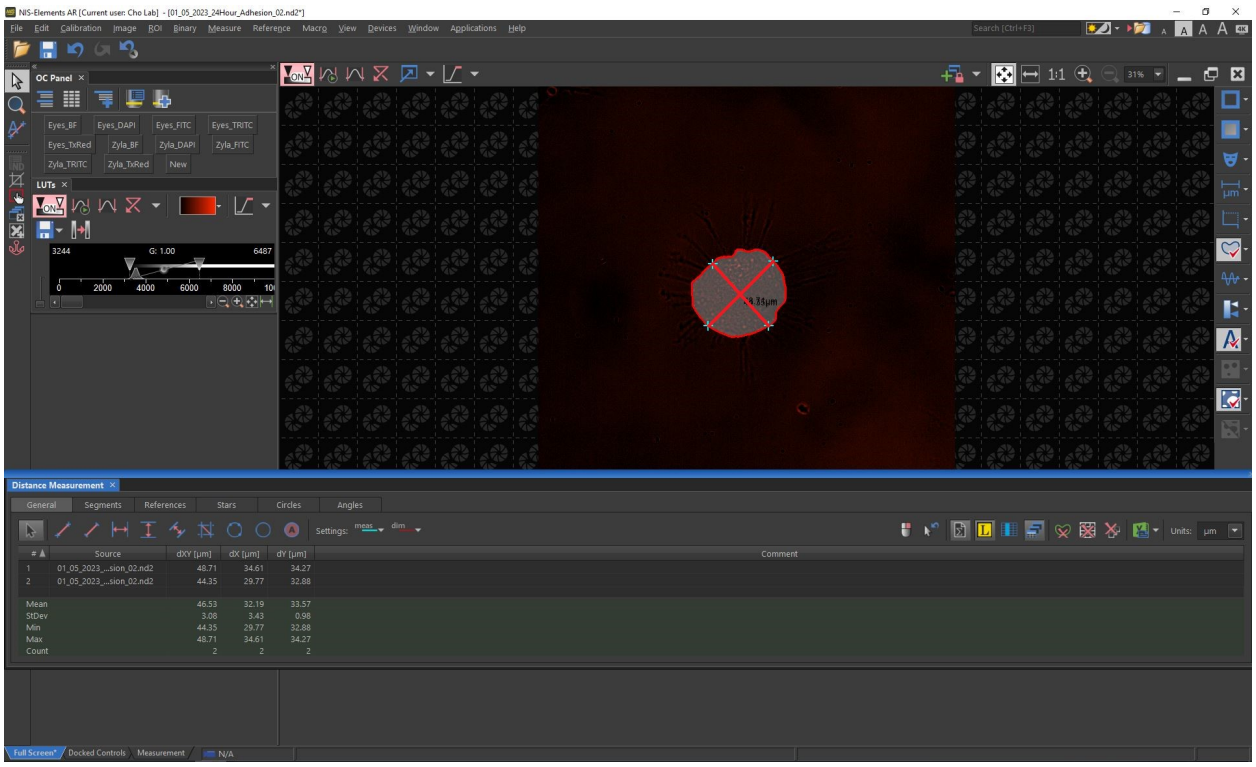

Figure 3-1: Example adipose-derived stem cell (ADSC) boundary marking and major/minor axis measurement. The cell boundary and both axes were manually marked. The cell boundary was marked using the ROI feature of the software. This featured displays the area in μm^2. Both axes were measured using the Measurement function.

3.4 Statistical Analysis

Due to the wide variance of cell size, Grubbs' test was performed to remove several outliers from the collected data. In the short time window samples, one observation was removed from each of hours 4, 6, 12, and 24. In the longer time window samples, one observation was removed from each of days 10 and 12. These six observations were separately analyzed to determine potential characteristics that are unique to the excluded cells. No such characteristics or correlation were observed and therefore were not further considered.

Student's t test was used to confirm a significant difference between sample means in eccentricity and area in the short time window samples. Student's t test was also used to compare the day 5 sample values to those of the following days.

The analyzed cell culture dishes in the longer-window had a sample size of at least 8 cells and the experiment was run twice, for a total of 16 measurements per timepoint. The green fluorescence within each image was divided by the length of individual actin filaments, and this value was normalized by the cell number. Normalization was needed because the high density of cells in each image made delineating individual cell boundaries nearly impossible. This value was then plotted against time (in days).

CHAPTER 4:

Results

4.1 Actin Filaments in Adipose-Derived Stem Cells

The experimental design was implemented to elucidate two specific aims. The first is to show and quantify the changes in cellular morphology and nascent stress actin filament arrangements of ADSCs during the first 24 hours after seeding. This is accomplished using two parameters, cellular area and cellular eccentricity. The eccentricity of a stem cell has been correlated in previous studies with overall cell health, viability, and progress of differentiation.[26,27,28] These studies have primarily focused on longer-term differentiation, and more investigation is needed into an earlier timeframe.

The second specific aim is to visualize and quantify the change of actin filament organization and morphology during longer-term adipogenic differentiation. While there is an abundance of research available examining the role of actin filaments in stem cell differentiation, little has been said specifically about stress actin filaments in ADSCs.[29,30, 31, 32]

4.2 Short-Term Cell Adhesion

The first specific aim of this study is to observe and quantify cellular behavior in the early window (<24 hours) of ADSC adipogenic differentiation. This behavior was quantified using 2 markers: cellular area and eccentricity. Composite images were created for hours 2, 4, 12, and 24 (Figure 4-1). One cell was centered in the field of view at 60x magnification for each timepoint. Visible within all cells observed at these times were punctate red marks, consistent with newly growing actin filaments that have not yet been evolved to stress fibers. Qualitative examination shows that cells at 2 and 4 hours are approximately round in shape and progress

toward a more linear shape as time approaches 24 hours. Additionally, cells are approximately 10 – 15 µm in diameter at hour 2 and grow to multiple times this size as adhesion progresses.

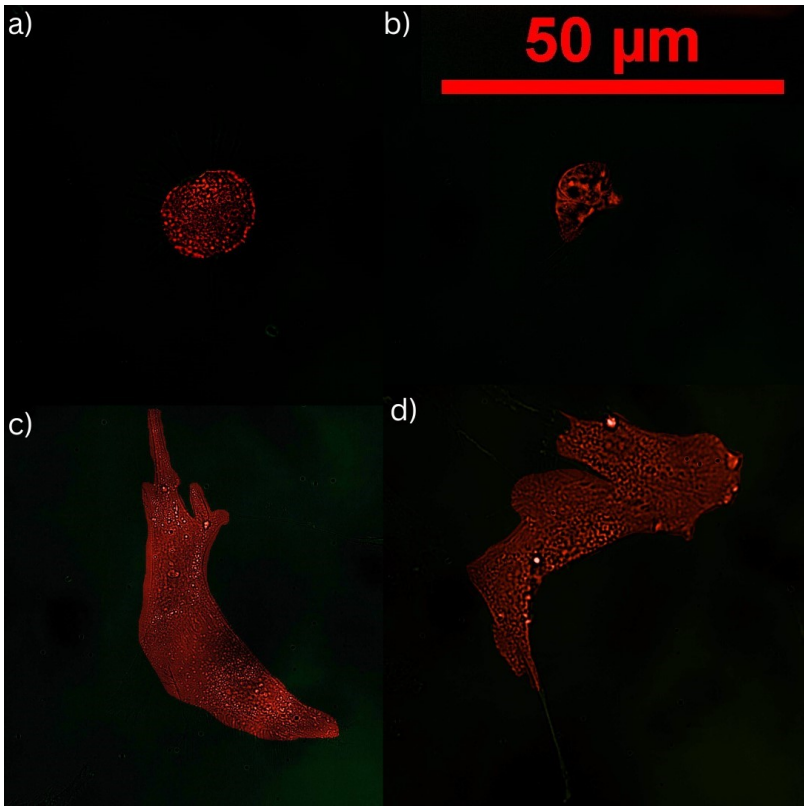

Figure 4-1: Single ADSC viewed at 60x magnification at various times post-seeding. All images were produced at 60x magnification. Nascent actin filaments are show in red via phalloidin x Texas Red stain. a) 2 hours: Cells have recently attached and are round in shape (eccentricity ~1) under microscope. b) 4 hours: Cells are still generally round but begin to increase in area. c) 12 hours: From hour 4 to hour 12, cellular area nearly triples, and eccentricity decreases. d) 24 hours: Increase of cellular area effectively stops, and eccentricity is approximately half that of hour 12. At the later timepoints, each cell has dozens of processes extending from the main cell body, causing a large variation in both eccentricity and area.

Quantitative analysis confirms these observations, as eccentricity is shown to decrease from hour 2 to 4. Following this period, eccentricity decreases rapidly as time post-seeding approaches 24 hours (Figure 4-2). Cellular area follows a somewhat opposite trend, as this measurement increases nearly three-fold from hour 2 to 4 and, with the magnitude of the increase tapering off to near zero around the 24 hour time point (Figure 4-3). An exponential curve was fitted to both the eccentricity and area data, and these were plotted as shown in Figure 4-4.

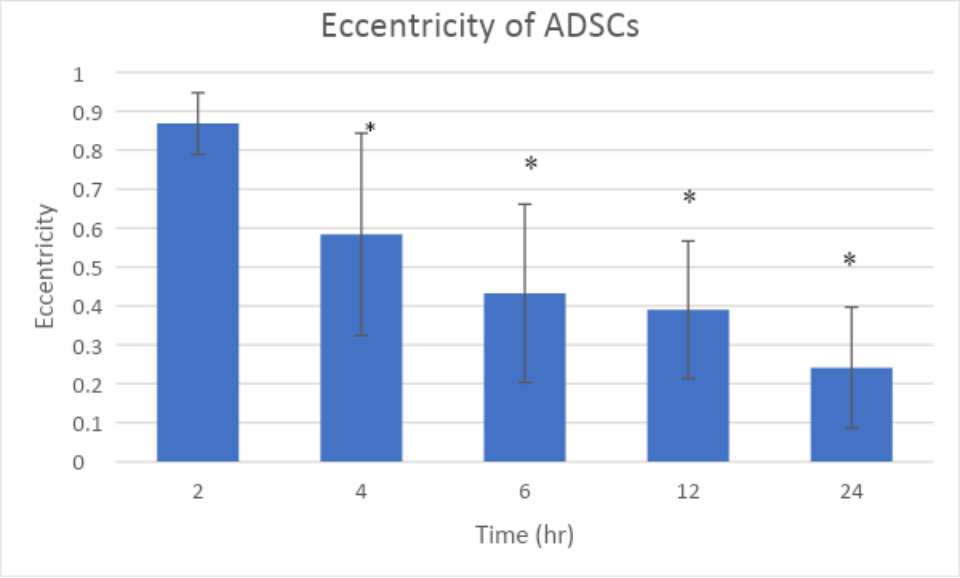

Figure 4-2: Calculated eccentricity of ADSCs within 24 hours post-seeding according to Equation 1. Eccentricity greatly decreases from hour 2 to hour 4, with the decrease continuing at a slower rate in the following timepoints. Each data point represents average ± SD of at least 10 cells from 2 independent experiments. *$p < 0.05$ compared to hour 2.

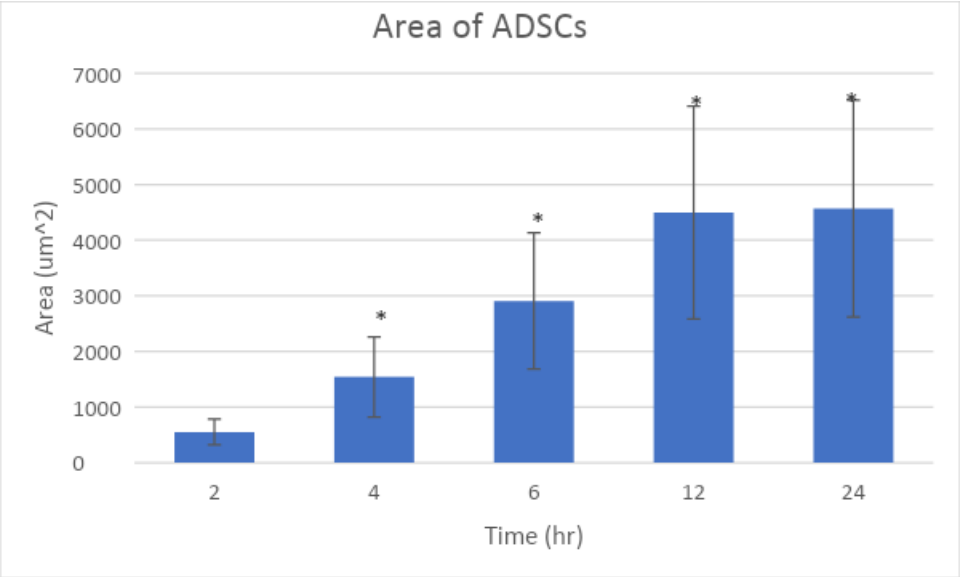

Figure 4-3: Measured area of ADSCs (+/- S.D.) within 24 hours post-seeding. There is a marked increase between one timepoint and the subsequent timepoint up to hour 12. Between hours 12 and 24, the increase plateaus. Each data point represents average ± SD of at least 10 cells from 2 independent experiments. *$p < 0.05$ compared to hour 2.

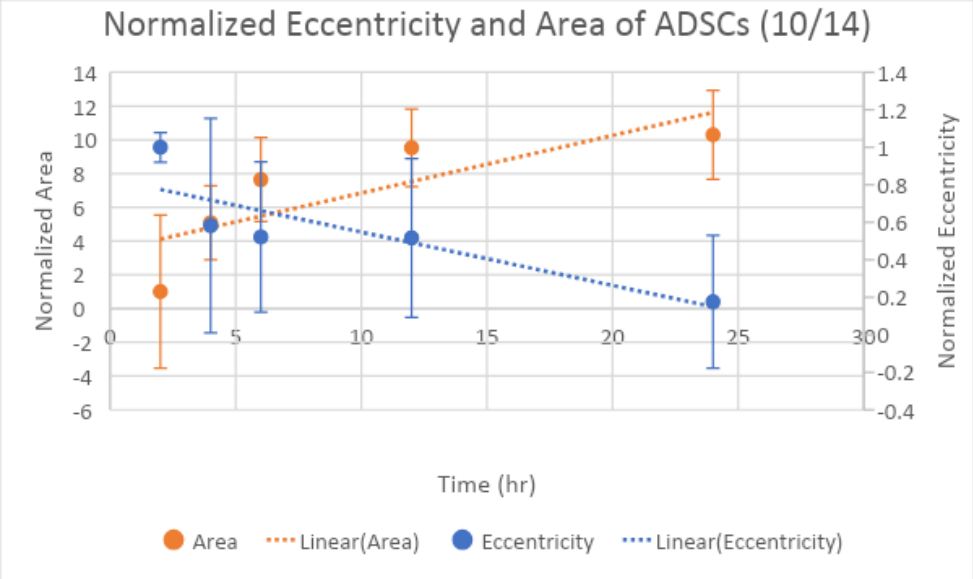

Figure 4-4: Normalized measured eccentricity and area of ADSCs within 24 hours post seeding. Normalization is necessary due to the high variability in cell size and eccentricity making comparison to hour 2 difficult. The best fit curve for both data sets is exponential. The two curves intersect at approximately 6 hours following the initial cell seeding. Each data point represents average ± SD of at least 10 cells from 2 independent experiments. *$p < 0.05$ compared to hour 2.

4.3 Longer-term Cell Differentiation

Previous studies have followed adipogenesis using the described induction media over about a two-week period. To date, there is a lack of study on stress actin filaments in ADSC over this time period. This study was designed to fill this gap. On the appropriate days, fluorescence of individual stress actin filaments was visualized, and representative filaments were selected manually to measure. Green fluorescence intensity was used as a measure of lipid formation throughout the experiment. An example image of actively differentiating ADSCs on day 10 is

shown in Figure 4-5. Of note in this image is the location of the actin filaments at the periphery of the cells. Filament lengths were measured using the Measurement feature in the Nikon NIS-Elements software and plotted against time as shown in Figure 4-6. An exponential curve was fitted to this data and has an r^2 value of 0.9223. An attempt at a linear fit was made for this data but this linear fit showed a lower r^2 value compared to an exponential fit. The overall green fluorescence intensity of lipid accumulation was normalized by the length of the actin filaments, and this number was further normalized by cell count for each day's samples. This subsequent value was plotted against time as shown in Figure 4-7. Another exponential curve was fitted to this data and has an r^2 value of 0.9978.

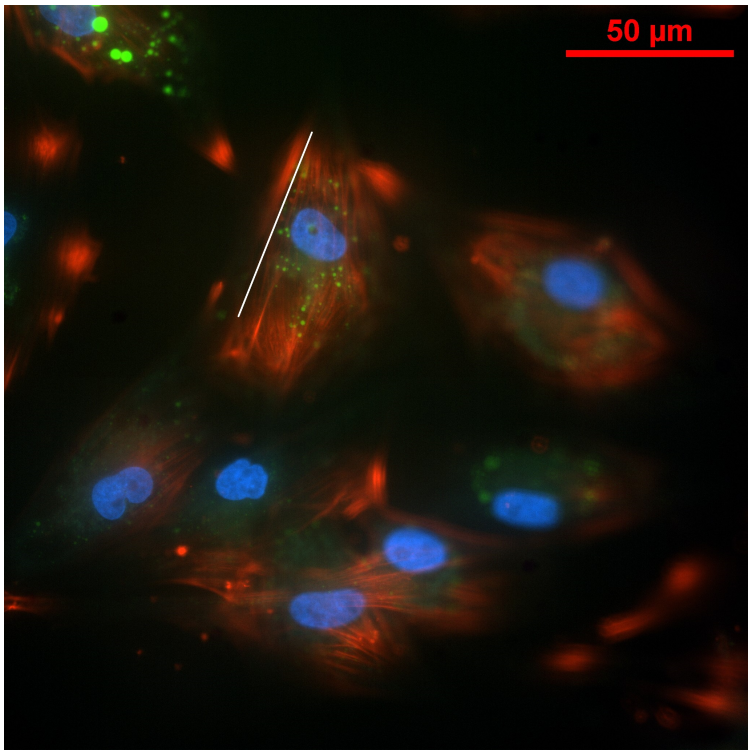

Figure 4-5: ADSCs at 60x magnification 5 days after seeding. No data was collected between hour 24 and day 5 due to experimental limitations. Nuclei are stained blue, actin filaments are stained red, and lipids are stained green. The white bar is parallel to and just below a single actin

filament used for calculations. After 5 days, actively differentiating cells begin to lose the linear shape seen after 24 hours and can be seen to begin rounding.

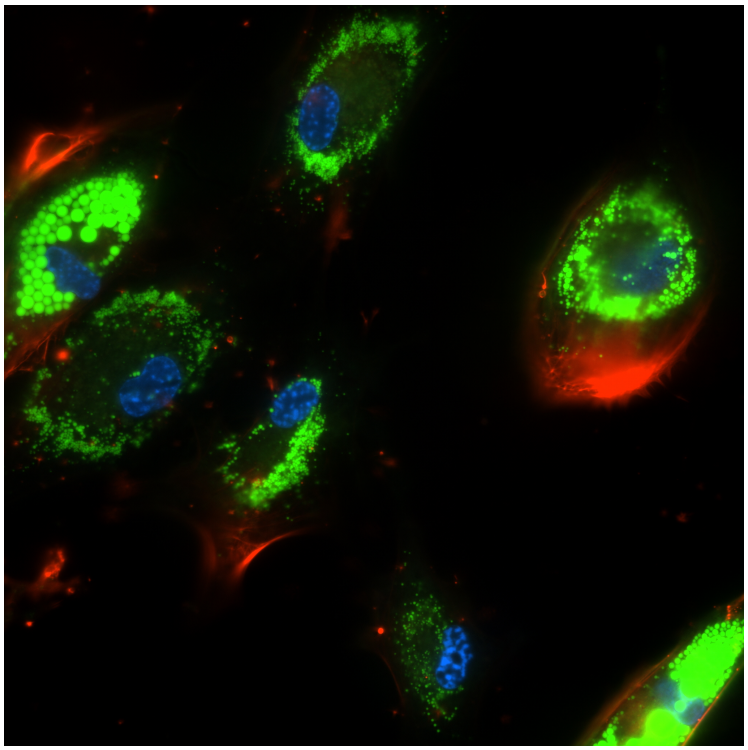

Figure 4-6: ADSCs at 60x magnification 10 days after seeding. Nuclei are stained blue, actin filaments are stained red, and lipids are stained green.

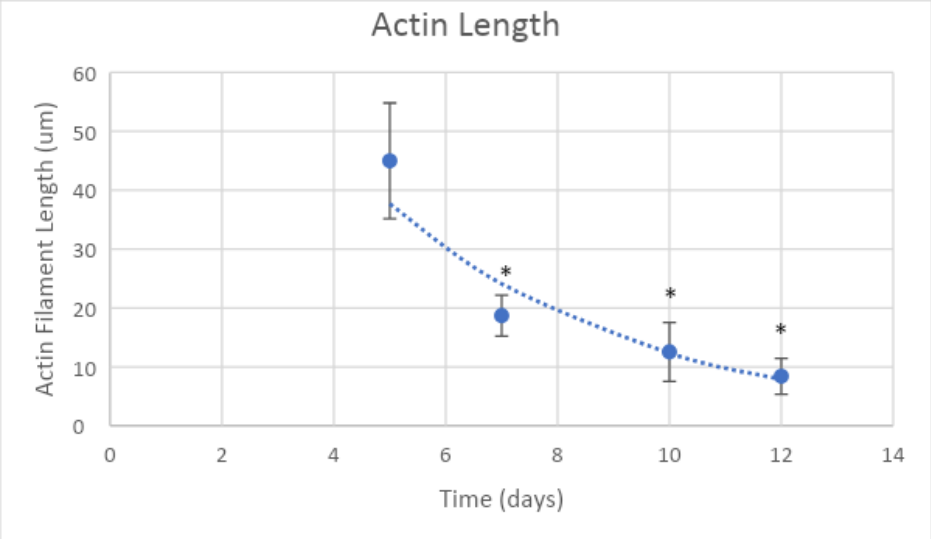

Figure 4-7: Actin filament length across 12 days of differentiation measured using NIS-Elements software. An exponential curve was fitted to this data. The length begins at day 5 around 30 µm and decreases approximately according to the curve until day 12. Actin length decreases over this period because ADSCs are becoming rounder. Each data point represents average ± SD of at least 8 cells from 3 independent experiments.

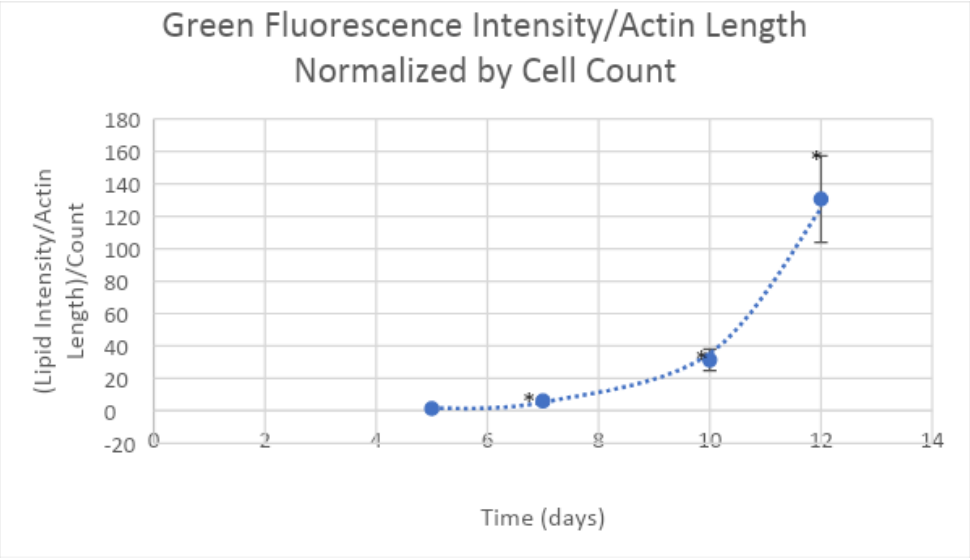

Figure 4-8: Experimental lipid accumulation divided by actin filament length, normalized by cell count across 12 days of differentiation. Lipid accumulation was found using LipidTox™.

Normalization was needed as eccentricity could not be found due to high cell density, which prevented identification of each cell's boundary. Each data point represents average ± SD of at least 8 cells from 3 independent experiments.

CHAPTER 5:

Conclusion

5.1 Aims of Thesis

There were two specific aims of this study. The first was to visualize, via nascent actin filament fluorescence, ADSC morphology and changes in a short (under 24 hour) window. This was done because work on the early phase of ADSC adhesion prior to differentiation is not readily available in the literature. Such a gap in knowledge provides room for further investigation into this process. Due to F-actin's critical role in cell adhesion, it presents itself as a prime candidate for a marker of this process. Improvements in substrate choice, growth conditions, and choice of induction molecules could streamline later differentiation efforts.[33, 34]

The second specific aim was to monitor and relate morphological changes to internal stress actin structures to adipogenic differentiation of ADSCs. Stem cells necessarily undergo drastic changes in morphology during the process of differentiation and F-actin is known to play a crucial role in this process.[35, 36] Therefore, quantification of these changes may provide new insight into the mechanisms involved.

5.2 Short-Term Cell Adhesion

Eccentricity as used in this study is defined as the length of a cell's minor axis divided by its major axis. A cell that is a perfect circle has an eccentricity of one, while a theoretically completely straight line would have an eccentricity approaching zero. As shown in Figures 4-2 and 4-4, ADSC eccentricity at hour 2 is approximately one. The quick drop in eccentricity at hour 4 is followed by a slower decrease in the subsequent hours. This is evidence that cells begin

the adhesion process with an area approximating a circle and become significantly more linear as time after seeding approaches 24 hours, as seen in Figure 4-1.

Of note in these results is the rather large error bar size in the measurements for hours 4, 6, 12, and 24. As cells are given more time to adhere to the given substrate, they begin to develop and extend processes outward from the main cellular body. These processes lead to a wide variety of possible cellular morphologies that, comparable to cells given less time to adhere, are linear. This is phenomenon is seen in Figure 4-1.

The observed linear increase of cellular area implies that once cells adhere to a surface, the increase is mostly steady. Future work with this data may focus on actin filaments and their role in the attachment during this early growth phase. More investigation is needed to elucidate the reasons for the eventual decrease in growth rate and the implications for eventual differentiation efforts. While this was not explored in this study, the results from this work are expected to provide a framework for properly interpreting and correlating stem cells' morphology with its potency.

5.3 Actin Morphology in Longer-Term ADSC Differentiation

While previous studies have shown that actin depolymerizes during adipogenic differentiation, very little work has been done to quantify its progress. Data collected in this research has done just this, demonstrating that as differentiation progresses, the length of actin filaments decreases rapidly over 12 days. This decrease is nearly four-fold from the length found in day 5 cells. Furthermore, the actin length can be related to lipid formation within the cells. The decrease in actin length, when lipid accumulation is taken into account as a measure of differentiation progress, is indicative of cellular rounding. This second rounding (the first being

the initial shape of the cells at hour 2) is where most of the lipid is being packed within the cells and most differentiation takes place.

Experimental data are needed to validate a mechanobiology model that is being developed in collaboration with Dr. Alan Bowling's group in Mechanical and Aerospace Engineering. The current study has provided data toward this work and has laid a framework for properly interpreting and correlating stem cell morphology with its potency.

5.4 Future Work

In future studies, measuring overall actin content within the cells may be a better indicator of actin morphological changes during differentiation, alternative to the filament length measurement used in this study. Additionally, mapping the location of individual actin filaments throughout this process could give better visualization of the changing arrangements during differentiation.

As shown throughout this study, actin filament morphology proves to be dynamic throughout the differentiation process. Necessarily, focal adhesions associated with the filaments would also change their arrangement, and likely their morphology as well. Future work would elucidate said changes.

Finally, utilization of genetic analysis of representative ADSCs as they differentiate could provide more evidence in addition to the green lipid fluorescence analysis used in this study. Quantitative analysis of the expression of genes such as PPARG and SREBP1 (major genes involved in adipogenesis) that would better demonstrate differentiation progress[37] should be included in the overall analyses, correlation and quantification of adipogenic differentiation.

References:

1. Tsuji W, Rubin JP, Marra KG. Adipose-derived stem cells: Implications in tissue regeneration. World J Stem Cells. 2014 Jul 26;6(3):312-21. doi: 10.4252/wjsc.v6.i3.312.

2. Park, I.-S., Han, M., Rhie, J.-W., Kim, S. H., Jung, Y., Kim, I. H., & Kim, S.-H. (2009). The correlation between human adipose-derived stem cells differentiation and cell adhesion mechanism. *Biomaterials*, *30*(36), 6835–6843. https://doi.org/10.1016/j.biomaterials.2009.08.057

3. Kilian, K. A., Bugarija, B., Lahn, B. T., & Mrksich, M. (2010). Geometric cues for directing the differentiation of mesenchymal stem cells. *Proceedings of the National Academy of Sciences*, *107*(11), 4872–4877. https://doi.org/10.1073/pnas.0903269107

4. Si, Z., Wang, X., Sun, C., Kang, Y., Xu, J., Wang, X., & Hui, Y. (2019). Adipose-derived Stem Cells: Sources, potency, and implications for regenerative therapies. *Biomedicine & Pharmacotherapy*, *114*, 108765. https://doi.org/10.1016/j.biopha.2019.108765

5. Titushkin, I., Sun, S., Paul, A., & Cho, M. (2013). Control of adipogenesis by Ezrin, radixin and Moesin-dependent biomechanics remodeling. *Journal of Biomechanics*, *46*(3), 521–526. https://doi.org/10.1016/j.jbiomech.2012.09.027

6. Tang, Q. Q., & Lane, M. D. (2012). Adipogenesis: From stem cell to adipocyte. *Annual Review of Biochemistry*, *81*(1), 715–736. https://doi.org/10.1146/annurev-biochem-052110-115718

7. Cooper GM. The Cell: A Molecular Approach. 2nd edition. Sunderland (MA): Sinauer Associates; 2000. Structure and Organization of Actin Filaments

8. Oliver-De La Cruz, J., Nardone, G., Vrbsky, J., Pompeiano, A., Perestrelo, A. R., Capradossi, F., Melajová, K., Filipensky, P., & Forte, G. (2019). Substrate mechanics controls adipogenesis through yap phosphorylation by dictating cell spreading. *Biomaterials*, *205*, 64–80. https://doi.org/10.1016/j.biomaterials.2019.03.009

9. Fu, Y., Luo, N., Klein, R. L., & Garvey, W. T. (2005). Adiponectin promotes adipocyte differentiation, insulin sensitivity, and lipid accumulation. *Journal of Lipid Research*, *46*(7), 1369–1379. https://doi.org/10.1194/jlr.m400373-jlr200

10. Sliogeryte, K., Thorpe, S. D., Lee, D. A., Botto, L., & Knight, M. M. (2014). Stem cell differentiation increases membrane-actin adhesion regulating cell blebability, migration and Mechanics. *Scientific Reports*, *4*(1). https://doi.org/10.1038/srep07307

11. Tojkander S, Gateva G, Lappalainen P. Actin stress fibers--assembly, dynamics and biological roles. J Cell Sci. 2012 Apr 15;125(Pt 8):1855-64. doi: 10.1242/jcs.098087.

12. Lieleg, O., Claessens, M. M., & Bausch, A. R. (2010). Structure and dynamics of cross-linked actin networks. *Soft Matter*, *6*(2), 218–225. https://doi.org/10.1039/b912163n

13. Maly, I. V., & Borisy, G. G. (2001). Self-organization of a propulsive actin network as an evolutionary process. *Proceedings of the National Academy of Sciences*, *98*(20), 11324–11329. https://doi.org/10.1073/pnas.181338798

14. Dominguez, R., & Holmes, K. C. (2011). Actin structure and function. *Annual Review of Biophysics*, *40*(1), 169–186. https://doi.org/10.1146/annurev-biophys-042910-155359

15. Sun, X., & Alushin, G. M. (2022). Cellular force‐sensing through actin filaments. *The FEBS Journal*, *290*(10), 2576–2589. https://doi.org/10.1111/febs.16568

16. NAUMANEN, P., LAPPALAINEN, P., & HOTULAINEN, P. (2008). Mechanisms of actin stress fibre assembly. *Journal of Microscopy*, *231*(3), 446–454. https://doi.org/10.1111/j.1365-2818.2008.02057.x

17. Narita, A., Oda, T., & Maéda, Y. (2011). Structural basis for the slow dynamics of the actin filament pointed end. *The EMBO Journal*, *30*(7), 1230–1237. https://doi.org/10.1038/emboj.2011.48

18. Yamashiro, S., Gokhin, D. S., Kimura, S., Nowak, R. B., & Fowler, V. M. (2012). Tropomodulins: Pointed‐end capping proteins that regulate actin filament architecture in diverse cell types. *Cytoskeleton*, *69*(6), 337–370. https://doi.org/10.1002/cm.21031

19. Carlier, MF., Shekhar, S. Global treadmilling coordinates actin turnover and controls the size of actin networks. *Nat Rev Mol Cell Biol* **18**, 389–401 (2017). https://doi.org/10.1038/nrm.2016.172

20. Edwards, M., Zwolak, A., Schafer, D. *et al.* Capping protein regulators fine-tune actin assembly dynamics. *Nat Rev Mol Cell Biol* 15, 677–689 (2014). https://doi.org/10.1038/nrm3869

21. Edwards, M., Zwolak, A., Schafer, D. *et al.* Capping protein regulators fine-tune actin assembly dynamics. *Nat Rev Mol Cell Biol* **15**, 677–689 (2014). https://doi.org/10.1038/nrm3869

22. Mahla, R. S. (2016). Stem cells applications in regenerative medicine and disease therapeutics. *International Journal of Cell Biology*, *2016*, 1–24. https://doi.org/10.1155/2016/6940283

23. Ruiz-Ojeda, F., Rupérez, A., Gomez-Llorente, C., Gil, A., & Aguilera, C. (2016). Cell models and their application for studying adipogenic differentiation in relation to obesity:

24. A Review. *International Journal of Molecular Sciences*, *17*(7), 1040. https://doi.org/10.3390/ijms17071040

25. Kim, I., Bang, S. I., Lee, S. K., Park, S. Y., Kim, M., & Ha, H. (2014). Clinical implication of allogenic implantation of adipogenic differentiated adipose-derived stem cells. *Stem Cells Translational Medicine*, *3*(11), 1312–1321. https://doi.org/10.5966/sctm.2014-0109

26. Lombardo, E., DelaRosa, O., Mancheño-Corvo, P., Menta, R., Ramírez, C., & Büscher, D. (2009). Toll-like receptor–mediated signaling in human adipose-derived stem cells: Implications for immunogenicity and immunosuppressive potential. *Tissue Engineering Part A*, *15*(7), 1579–1589. https://doi.org/10.1089/ten.tea.2008.0340

27. McIlwain, D.L., Hoke, V.B. The role of the cytoskeleton in cell body enlargement, increased nuclear eccentricity and chromatolysis in axotomized spinal motor neurons. *BMC Neurosci* 6, 19 (2005). https://doi.org/10.1186/1471-2202-6-19

28. Kannan, N., & Beers, P. (Eds.). (2022). Stem cell assays. *Methods in Molecular Biology*, *2429*, 455–471. https://doi.org/10.1007/978-1-0716-1979-7

29. Szczepankiewicz, F., van Westen, D., Englund, E., Westin, C.-F., Ståhlberg, F., Lätt, J., Sundgren, P. C., & Nilsson, M. (2016). The link between diffusion MRI and tumor heterogeneity: Mapping cell eccentricity and density by diffusional variance decomposition (divide). *NeuroImage*, *142*, 522–532. https://doi.org/10.1016/j.neuroimage.2016.07.038

30. Chen, L., Hu, H., Qiu, W., Shi, K., & Kassem, M. (2018). Actin depolymerization enhances adipogenic differentiation in human stromal stem cells. *Stem Cell Research*, *29*, 76–83. https://doi.org/10.1016/j.scr.2018.03.010

31. Fan, Y.-L., Zhao, H.-C., Li, B., Zhao, Z.-L., & Feng, X.-Q. (2019). Mechanical roles of F-actin in the differentiation of Stem Cells: A Review. *ACS Biomaterials Science & Engineering*, *5*(8), 3788–3801. https://doi.org/10.1021/acsbiomaterials.9b00126

32. Weber, G. F., & Menko, A. S. (2006). Actin filament organization regulates the induction of Lens cell differentiation and survival. *Developmental Biology*, *295*(2), 714–729. https://doi.org/10.1016/j.ydbio.2006.03.056

33. Fan, Y.-L., Zhao, H.-C., Li, B., Zhao, Z.-L., & Feng, X.-Q. (2019). Mechanical roles of F-actin in the differentiation of Stem Cells: A Review. *ACS Biomaterials Science & Engineering*, *5*(8), 3788–3801. https://doi.org/10.1021/acsbiomaterials.9b00126

34. Wang, Y., & Chen, C. S. (2013). Cell adhesion and mechanical stimulation in the regulation of mesenchymal stem cell differentiation. *Journal of Cellular and Molecular Medicine*, *17*(7), 823–832. https://doi.org/10.1111/jcmm.12061

35. Lv, H., Li, L., Sun, M., Zhang, Y., Chen, L., Rong, Y., & Li, Y. (2015). Mechanism of regulation of stem cell differentiation by matrix stiffness. *Stem Cell Research & Therapy*, *6*(1). https://doi.org/10.1186/s13287-015-0083-4

36. Sen, B., Uzer, G., Samsonraj, R. M., Xie, Z., McGrath, C., Styner, M., Dudakovic, A., van Wijnen, A. J., & Rubin, J. (2017). Intranuclear actin structure modulates mesenchymal stem cell differentiation. *Stem Cells*, *35*(6), 1624–1635. https://doi.org/10.1002/stem.2617

37. Ambriz, X., de Lanerolle, P., & Ambrosio, J. R. (2018). The mechanobiology of the actin cytoskeleton in stem cells during differentiation and interaction with biomaterials. *Stem Cells International*, *2018*, 1–11. https://doi.org/10.1155/2018/2891957

38. Dahlman I, Arner P. Genetics of adipose tissue biology. Prog Mol Biol Transl Sci. 2010;94:39-74. doi: 10.1016/B978-0-12-375003-7.00003-0.